LARGE SCALE WATER BASED ORGANIC PHOTOVOLTAICS

Júlia Ketzer Majewski[1], Maiara de Jesus Bassi[2], and Lucimara Stolz Roman[3]

[1] PhD Student, Department of Physics, UFPR, Curitiba (Brazil)

[2] PhD, Department of Physics, UFPR, Curitiba (Brazil)

[3] Professor, Department of Physics, UFPR, Curitiba (Brazil)

Abstract

With increasing energy demand and the depletion of fossil fuels, the development of sustainable energy technologies is critical. Organic Photovoltaic Devices (OPVs) offer advantages such as flexibility, low cost, and scalability; however, their fabrication often relies on toxic organic solvents, raising environmental concerns. This study explores the use of water-based polymer nanoparticle (NP) inks as a safer alternative for OPV active layers. Donor and donor:acceptor nanoparticle formulations, including fullerene and non-fullerene systems, were processed via slot die, blade, and spin coating to produce homogeneous films. These were analyzed optically, morphologically, electrically, and chemically. Results showed that nanoparticle inks can yield stable OPVs, with enhanced environmental performance and long-term stability confirmed under ISOS-L-2 testing protocols.

Keywords: Organic Photovoltaics, Polymer Nanoparticles, Eco-friendly Conductive Ink.

1. Introduction

Organic photovoltaics (OPVs) have emerged as a promising class of light-weight, mechanically compliant and solution-processable photovoltaic technologies with potential for low-energy, roll-to-roll manufacturing and integration in large-area applications in the built environment. Although competitive power conversion efficiencies have been achieved in recent years, largely due to morphologically optimized bulk-heterojunctions incorporating non-fullerene acceptors (NFAs), state-of-the-art device fabrication remains dominantly reliant on high-volatility and toxic aromatic chlorinated solvents such as chlorobenzene or chloroform, raising concerns related to worker safety, industrial handling, flammability, end-of-life environmental release, and overall life-cycle sustainability.

The development of water-based semiconductor inks constitutes a compelling route to address these intrinsic solvent liabilities, enabling processing under benign conditions without compromising morphology, absorption or electronic function according to Bassi et al. (2025). Miniemulsion synthesis routes have been shown to yield semiconducting nanoparticles (NPs) with controlled physico-chemical attributes including size, surface charge, and colloidal stability, compatible with scalable coating methods such as blade and slot-die. When used as active layers, water-based polymer nanoparticles (NPs) can mitigate morphological coarsening and photodegradation pathways relative to solvent-cast analogs, thereby extending the operational stability of OPVs.

Here we report the synthesis, processing and device integration of water-based polymer nanoparticles (NPs) prepared from donor-only (F8T2) and binary donor:acceptor blends (F8T2:PCBM and F8T2:ITIC), and subsequently deposited via scalable coating techniques. We correlate colloidal (DLS, ZP), morphological (AFM roughness and SEM), optical (UV–Vis, PL) and device-level (J–V under ISOS-L-2 with and without light) metrics to make a direct comparative evaluation against conventional chloroform-processed reference films. We further discuss the emergent advantages associated with the transition from fullerene to NFA-based aqueous NPs in terms of spectral coverage, photogeneration, charge-transfer efficacy and stability under stress. Our findings establish water-based NP inks as a technologically viable and environmentally safer replacement for conventional solvent-cast active layers in large-area organic photovoltaics.

2. Experimental Procedure

Selection and/or peer review under responsibility of Scientific Committee
10.18086/swc.2025.03.38 Available at http://proceedings.ises.org

Poly(9,9-dioctylfluorene-alt-bithiophene) (F8T2), phenyl-C61-butyric acid methyl ester (PCBM) and the non-fullerene acceptor ITIC were used as received without additional purification. Sodium dodecyl sulfate (SDS) served as surfactant in the aqueous phase during miniemulsion synthesis. All aqueous dispersions were prepared using deionized water. Chloroform (CF)-processed films were fabricated as reference controls using conventional solution deposition with equivalent solid contents into otherwise identical device architectures.

Water-based polymer nanoparticles (NPs) were produced via a miniemulsion route as reported by Landfester et al. (1999), illustrated in **figure 1**, in which the hydrophobic donor or donor:acceptor semiconductors were first dissolved in a chloroform organic phase, followed by emulsification in an aqueous SDS solution under vigorous stirring to generate a macroemulsion. Subsequent probe ultrasonication led to the formation of a kinetically stabilized miniemulsion. The residual organic solvent was fully removed by thermal evaporation, and excess surfactant was eliminated through dialysis against deionized water several times. Three dispersions were prepared: F8T2 NPs, F8T2:PCBM NPs and F8T2:ITIC NPs at final solid contents achieving 10–60 mg mL^{-1}.

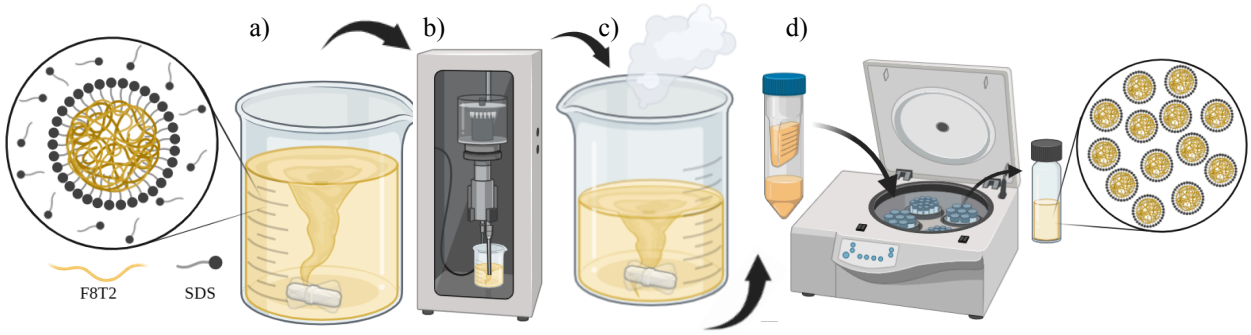

Fig 1: Illustration of the miniemulsion synthesis, representing the macroemultion (a), the sonication (b), the evaporation (c) and the dialysis (d) processes, resulting in water based nanoparticles.

Water-based polymer nanoparticle (NP) films were deposited on pre-cleaned glass or glass/FTO substrates using spin or blade coating under controlled shear conditions. Deposition parameters (gap height, coating speed and substrate temperature) were tuned to yield uniform films without secondary drying fronts or coffee-ring instabilities. Chloroform-cast references were prepared for direct benchmarking under identical substrate and post-processing conditions.

F8T2-based nanodispersions were integrated in inverted devices of the form glass/FTO/ZnO/NP-blend/MoO_3/Ag. All devices were tested under simulated AM 1.5G illumination at 100 mW cm^{-2}. Device performance under degradation was assessed in accordance with ISOS-L-2 conditions (60 °C, 80% RH, continuous light exposure).

Dynamic light scattering (DLS) was used to determine hydrodynamic diameter distributions and assess synthetic control over NP size. Zeta potential (ZP) measurements probed colloidal electrostatic stabilization. Film morphology and topography were quantified via scanning electron microscopy (SEM) and atomic force microscopy (AFM), reporting the root-mean-square roughness (Rq) extracted from step profiles. Optical absorption spectra were recorded using UV–Vis spectrophotometry, while steady-state photoluminescence (PL) experiments were used to quantify quenching efficiency for donor–acceptor electronic coupling and interfacial charge transfer. Device J–V curves were also collected.

3. Results and Discussion

F8T2-based nanoparticles, both neat and blended with PCBM or ITIC, were successfully synthesized using the established miniemulsion protocol, yielding stable colloidal dispersions with well-controlled size and uniform morphology. The optical response of the nanoparticle systems was examined by steady-state photoluminescence and UV–vis absorption, to reveal both exciton dynamics and packing-induced reorganization of the electronic structure. The photoluminescence spectra (**Figure 2a**) evidenced highly efficient exciton quenching in both blends relative to neat F8T2 nanoparticles, with the F8T2:ITIC formulation reaching up to 99.95% quenching efficiency, slightly exceeding that of the F8T2:PCBM analogue.

Complementarily, the UV–vis absorption spectra of F8T2 in **Figure 2b** reveal pronounced signatures of packing-driven reorganization already when comparing F8T2 in chloroform to the corresponding nanoparticle state. The nanoparticles show a clear red-shift of the main vibronic band together with a relative enhancement of the 0–0 vibronic peak, a spectral configuration widely recognized as a manifestation of strengthened excitonic coherence and increased through-space π–π coupling. The amplified 0–0/0–1 intensity ratio reflects a transition from a liquid-like molecularly disordered regime toward a more electronically coherent aggregate manifold, a transformation that is structurally enabled by the confined and kinetically modulated environment of the nanoparticle formation.

Crucially, these spectral signatures propagate into the donor:acceptor blends in the presence of both fullerene and non-fullerene acceptors, shown in **Figure 2c** and **2d**. In both F8T2:PCBM and F8T2:ITIC systems, the nanoparticle film spectra continue to exhibit the same red-shifted vibronic pattern with an elevated 0–0 transition, demonstrating that neither acceptor suppresses the aggregation-assisted excitonic order that emerges in the NP state. Instead, the blend spectra demonstrate that the donor packing remain electronically accessible and that the excitonic coupling regime that favors charge separation coexists with efficient quenching.

The extent of vibronic reorganization becomes even more pronounced in blade-coated films. In both blends, blade-coated layers show a further intensification of the 0–0 transition and a deeper red-shift than their spin-coated counterparts, consistent with the slower and more thermodynamically permissive drying intrinsic to blade meniscus coating. This process window enhances supramolecular relaxation and promotes more coherent donor packing than the kinetically abrupt spin-drying route. Taken together with the photoluminescence quenching in the blended nanoparticles, these absorption data show that the nanoparticle strategy not only tolerates but actually favours the emergence of electronically desirable packing under scalable deposition, preserving the excitonic pre-conditions necessary for efficient charge generation.

Overall, the combined photoluminescence and UV–vis results show that nanoparticle formulation does not degrade the interfacial electronic function of donor–acceptor blends. Instead, it preserves high interfacial quenching efficiency while amplifying the vibronic coherence that is spectroscopically correlated with improved exciton harvesting and charge transport. The fact that these attributes persist or even sharpen under blade coating provides compelling evidence that nanoparticle inks constitute a viable, scalable route for fabricating electronically high-quality blend layers without incurring the microstructural penalties often associated with non-equilibrium film formation.

Dynamic light scattering (DLS) was employed to determine the hydrodynamic size of neat F8T2 nanoparticles and their binary blends with PCBM and ITIC. All samples exhibited narrow distributions with mean diameters on the order of 50 nm (**Figure 3c**), consistent with the intended formulation window for organic semiconductor nanostructures to preserve the donor:acceptor interfaces within the exciton diffusion length. The F8T2 dispersion displayed an average hydrodynamic diameter centered at 50 nm with a low polydispersity index (PDI) of approximately 0.25, indicative of homogeneous size distribution and the absence of aggregation. Upon blending with PCBM or ITIC, the peak position remained within the same size regime, showing no statistically significant shift in hydrodynamic diameter, which suggests that neither acceptor perturbs the colloidal stability or packing-induced swelling of the polymer-rich domains under the preparation conditions used. The preserved monodispersity further indicates that interfacial interactions in the blends do not promote secondary agglomeration or coalescence at the dispersion stage. These results support that the nanostructured blends remain colloidally stable and size-defined, preserving the nanoscale dimensionality relevant for downstream optoelectronic or device processing steps.

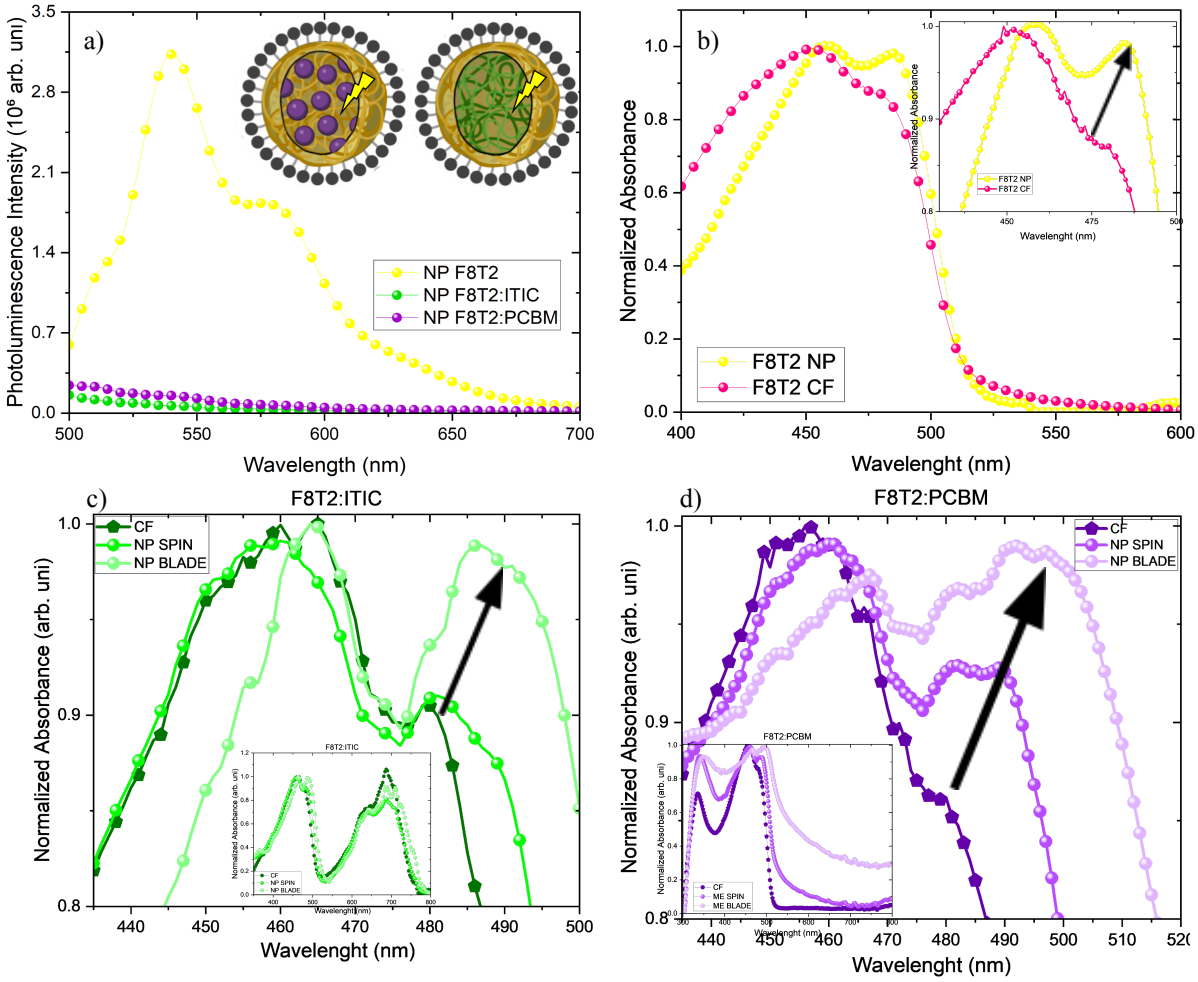

Fig 2: (a) Photoluminescence of the F8T2 based nanoparticles with illustration of the charge transfer occurring inside each nanoparticle; b) normalized absorbance of the neat F8T2 dissolved in chloroform and in nanoparticles with insert of the graphic focusing on the main two peaks, and normalized absorbance of the main bands of the blends for chloroform, and nanoparticles coated by spin and blade for F8T2:ITIC (c) and F8T2:PCBM (d), both with incept of the full graphics.

In line with the size stability, the zeta potential values confirmed strong electrostatic stabilization. The F8T2:PCBM nanoparticles achieved a zeta potential of −53.3 mV, whereas the F8T2:ITIC nanoparticles showed −33.7 mV. The presence of sufficiently high negative surface charge is a critical indicator that the nanoparticles are not only kinetically stabilized but also electrostatically protected against irreversible aggregation through repulsive double-layer interactions. From a mechanistic perspective, this stabilization is attributed to the adsorption of SDS at the NP–water interface, reducing the interfacial tension while imposing electrostatic repulsion between colloidal entities. This is important because, in the absence of adequate zeta potential magnitude, phase separation, sedimentation, and uncontrolled coalescence would occur during storage or coating, compromising film uniformity.

The observation that F8T2:PCBM and F8T2:ITIC nanoparticles exhibit different absolute ZP magnitudes is not incidental. The two acceptors differ not only in polarity and surface energy, but also in interfacial packing affinity for SDS, modifying the local hydration shell. These subtle but systematic shifts reveal that compositionally distinct donor:acceptor blends can modulate electrostatics at the colloidal interface without compromising dispersion stability. In this respect, water-based polymer nanoparticles (NPs) outperform traditional solvent-based inks, which are governed primarily by solvent evaporation kinetics rather than colloidal stability.

The morphology and surface properties of the nanoparticles were examined by scanning electron microscopy (SEM) and atomic force microscopy (AFM) to provide complementary insight into size, shape,

and topography. SEM images of the F8T2:PCBM and F8T2:ITIC nanoparticles in **Figure 3a** and **3b** respectively reveal highly spherical and well-defined nanoparticles with diameters centered around 50 nm, consistent with the scale observed by dynamic light scattering. The clear size uniformity and absence of significant aggregation indicate that the nanoparticle synthesis procedure yields discrete colloidal entities with well-controlled dimensions, which is in line with the DLS data previously discussed.

AFM imaging was then employed to investigate the topography of thin films deposited by different methods. For films prepared from donor:acceptor blends dissolved in chloroform, the surface is extremely smooth, exhibiting low root-mean-square roughness (Rq < 5 nm) for both F8T2:PCBM and F8T2:ITIC (**Figure 3d** and **3g**). By contrast, films spin-coated from nanoparticle dispersions display significantly higher roughness, with Rq values of 43.35 nm for F8T2:PCBM and 23.48 nm for F8T2:ITIC (**Figure 3e** and **3h**). The increase in surface roughness reflects the particulate nature of the films and the presence of discrete nanoscale domains on the surface. Moreover, when blade coating is employed, roughness values increase further, reaching 66.54 nm for F8T2:PCBM and 124.18 nm for F8T2:ITIC (**Figure 3f** and **3i**), highlighting the pronounced surface modulation that can be achieved in large-area, slow-drying deposition processes.

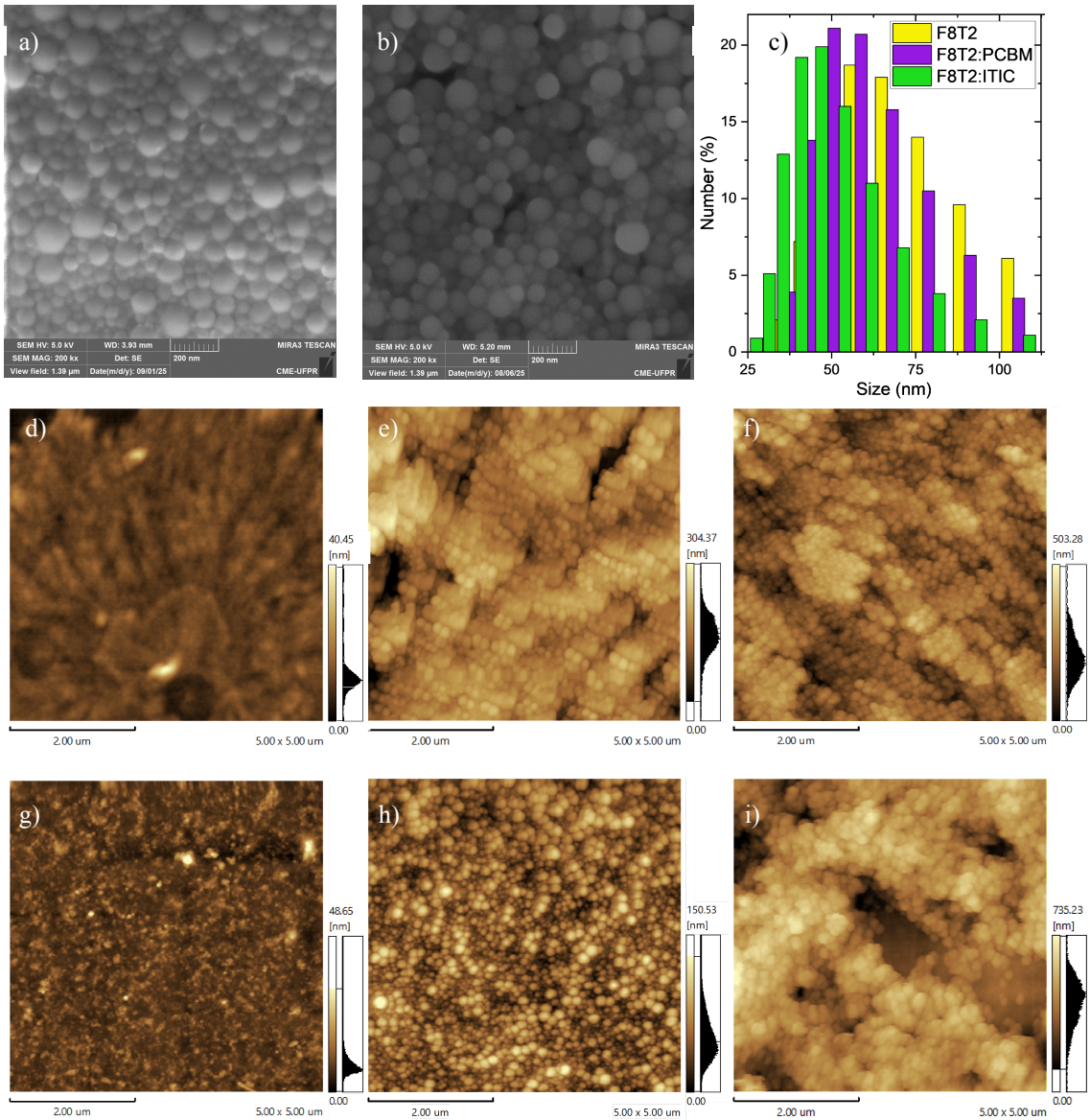

Fig 3: (a–b) SEM of nanoparticles for (a) F8T2:PCBM and (b) F8T2:ITIC. (c) Size distribution histogram from DLS measurements of the nanoparticles. (d–f) AFM topography images of F8T2:PCBM films: (d) spin-coated from chloroform solution, (e) spin-coated from nanoparticle dispersion, and (f) blade-coated from nanoparticle dispersion. (g–i) AFM topography images of F8T2:ITIC films: (g) spin-coated from chloroform solution, (h) spin-coated from nanoparticle dispersion, and (i) blade-coated from nanoparticle dispersion.

The observed increase in surface roughness in nanoparticle-based films is not merely a geometric consequence of the NP dimensions, but can have profound implications for organic photovoltaic (OPV) performance. Enhanced nanoscale topography can improve light scattering within the active layer, increasing optical path length and potentially enhancing photon absorption, according to de Jesus, et al. (2021). Additionally, the roughened morphology may facilitate more efficient donor–acceptor interfacial area, promoting exciton dissociation and charge separation. Nevertheless, excessive roughness could also introduce challenges in layer uniformity and electrode contact, emphasizing the importance of balancing nanoparticle-induced topographical features with device processing requirements. Overall, the AFM analysis demonstrates that nanoparticle formulations provide a tunable pathway to modulate film morphology and surface features, with clear advantages for scalable deposition methods such as blade coating, while preserving nanoscale size and uniformity.

The photostability of the nanoparticle dispersions was evaluated by monitoring the evolution of their UV–vis absorption spectra under continuous illumination following the ISOS-L-2 testing protocol without any encapsulation. As shown in **Figure 4a**, the absorption peak of the F8T2 nanoparticles degrades significantly more slowly than the correspondent dissolved in chloroform. This enhanced stability indicates that the nanoparticle formulation provides a protective effect, likely arising from the confined and aggregated polymer domains, which reduce the exposure of polymer sites to photo-oxidative processes and limit the diffusion of reactive species. The result demonstrates that nanoparticles can improve the intrinsic photostability of the active materials, an important attribute for long-term operational stability in organic photovoltaic devices.

Preliminary current–voltage (J–V) measurements **Figure 4b** reveal that both nanoparticle-based films exhibit a measurable photovoltaic response under standard illumination conditions, despite the modest power conversion efficiencies observed in these initial experiments. As expected from the enhanced charge-transfer interactions suggested by the optical characterization, the F8T2:ITIC nanoparticle devices show slightly higher short-circuit current and overall performance compared to the F8T2:PCBM analogue. These results confirm that the nanoparticle strategy preserves the ability of donor:acceptor blends to generate photocurrent and validates their potential for further optimization in device architectures. Taken together, the data highlight the dual advantage of nanoparticles: improved photostability and retention of functional photovoltaic behavior, particularly with non-fullerene acceptors that can exploit the favorable electronic coupling in the nanoparticle form.

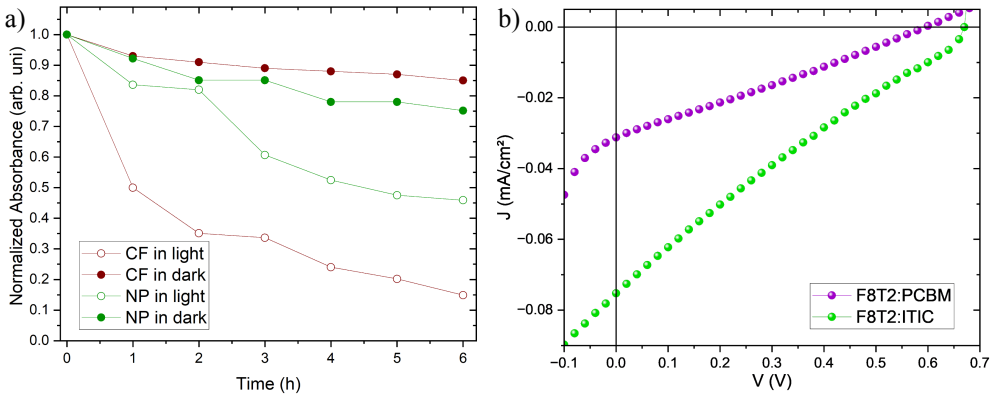

Fig 4: Photostability of F8T2 nanoparticles versus chloroform solutions under ISOS-L-2 testing protocols (a) and J–V curves showing measurable photovoltaic response for both NP blends (b).

In summary, the systematic characterization of F8T2-based nanoparticles demonstrates that the nanoparticle approach successfully preserves nanoscale size, enhances optical and morphological order, and provides improved photostability compared to conventional solution-processed blends. Despite modest initial device efficiencies, the nanoparticles maintain functional exciton quenching, coherent vibronic packing, and measurable photovoltaic response, with non-fullerene ITIC blends showing slightly superior performance as expected. The combined optical, morphological, and preliminary device data highlight the potential of nanoparticle formulations for scalable fabrication methods, such as blade coating, offering a promising pathway toward stable and electronically well-defined active layers for organic photovoltaics.

4. Conclusion

In this work, F8T2-based nanoparticles, both neat and blended with PCBM or ITIC, were successfully synthesized and comprehensively characterized, demonstrating precise control over size, morphology, and surface properties. Dynamic light scattering and SEM analyses confirmed that the nanoparticles possess well-defined spherical shapes with diameters around 50 nm, consistent across both blend types, while AFM revealed tunable surface roughness that can be modulated through deposition method, reaching significantly higher values under blade coating. These findings highlight the ability of nanoparticles to maintain structural uniformity while enabling morphological features beneficial for organic photovoltaic (OPV) applications, such as enhanced donor–acceptor interfacial area and light-scattering properties.

Optical analyses further revealed that nanoparticle formation preserves and even enhances desirable photophysical properties. UV–vis absorption spectra indicated red-shifted vibronic transitions and increased 0–0/0–1 ratios, signifying improved excitonic coherence and more ordered donor packing. Steady-state photoluminescence measurements demonstrated near-quantitative exciton quenching, particularly in F8T2:ITIC nanoparticles, consistent with enhanced interfacial electronic coupling. Together, these optical results show that the nanoparticle strategy does not compromise charge-transfer efficiency and can actually reinforce electronic ordering favorable for exciton dissociation and charge transport.

Finally, preliminary device testing and photostability studies underscore the technological promise of nanoparticle formulations. The nanoparticles exhibit slower degradation of absorption under continuous illumination and retain measurable photovoltaic response, with non-fullerene ITIC blends showing slightly superior performance. These combined structural, optical, and functional advantages demonstrate that nanoparticle-based inks represent a scalable, versatile, and electronically robust approach to active layer fabrication. Overall, this work motivates the further exploration of nanoparticles as a platform for high-performance, stable, and large-area OPV devices, bridging the gap between colloidal control and device-relevant functionality.

5. References

Bassi, M. J., Majewski, J.K., Roman, L.S., Colloids and solar energy interactions, Chapter from Riegel-Vidotti, I. C.; Zimmermann, L. M.; De Barros, H. R. (Ed.). Contribution of Colloidal Materials to Air, Water and Soil Environmental Sustainability: From Basic Concepts to Advanced Applications, Royal Society of Chemistry, 2025, https://doi.org/10.1039/9781837676149

de Jesus Bassi, M., Wouk, L., Renzi, W., Oliveira, C. K., Duarte, J. L., Heisler, I. A., & Roman, L. S. (2021). Non-radiative energy transfer in aqueously dispersed polymeric nanoparticles for photovoltaic applications. *Synthetic Metals*, *275*, 116740.

Landfester, K., Bechthold, N., Tiarks, F., & Antonietti, M. (1999). Formulation and stability mechanisms of polymerizable miniemulsions. *Macromolecules*, *32*(16), 5222-5228.

Ramoni, M., de Jesus Bassi, M., Wouk, L., Pacheco, K. R. M., Fernández, A. B., Renzi, W., ... & Roman, L. S. (2021). Morphology, photoexcitation dynamics and stability of water-dispersed nanoparticle films based on semiconducting copolymer. *Thin Solid Films*, *721*, 138536.